DOI:
10.1109/ISBI.2016.7493263

Document Version
Peer reviewed version

REGRESSION ANALYSIS FOR ASSESSMENT OF MYELINATION STATUS IN PRETERM BRAINS WITH MAGNETIC RESONANCE IMAGING

Siying Wang[1], *Maria Kuklisova-Murgasova*[2], *Joseph V. Hajnal*[2], *Christian Ledig*[3], *Julia A. Schnabel*[1,2]
[1]Department of Engineering Science, University of Oxford, UK
[2]Division of Imaging Sciences and Biomedical Engineering, Kings College London, UK
[3]Department of Computing, Imperial College London, UK

ABSTRACT

Myelination is considered an important developmental process during human brain maturation and to be closely correlated with gestational age. Assessment of the myelination status generally requires dedicated imaging, yet the conventional T_2-weighted acquisitions routinely obtained during clinical imaging of neonates carry signatures that are thought to be directly associated with myelination. In this work, we propose a method to identify these signatures which could potentially be used to assess brain maturation of preterm neonates directly from T_2-weighted magnetic resonance images. First we segment the tissue that is likely to contain myelin from 96 preterm neonates. We then construct a spatio-temporal atlas based on the registered segmentations by fitting a voxelwise logistic regression model. Finally, the atlas is utilized to estimate the gestational ages of individual subjects in a leave-one-out procedure. The logistic model yields a root mean squared error of 10 days, as compared to 13 days for the ages predicted using a kernel regression atlas.

***Index Terms*—** Neonatal brain MRI, myelination, logistic regression, gestational age estimation

1. INTRODUCTION

Myelin is generally imaged with magnetization transfer imaging and multi-component relaxometry, but these dedicated scans are not normally performed during clinical imaging of neonates due to time constraints [1]. The aim of this paper is to propose a method to help assess the myelination status of preterm brains in a large-scale study using routinely acquired clinical magnetic resonance imaging (MRI).

Myelin bearing regions may be identified from the characteristic high intensities on T_1-weighted (T_1w) MR images, which are reversed in T_2w contrast [2]. However, the signal properties of these clinical MR images depend on many factors and myelinated white matter can have signal properties that are close to those of dense grey matter. To overcome this difficulty, we segment the tissue likely to contain myelin from 96 preterm neonates based on both intensity and spatial anatomical knowledge. We then construct a four-dimensional (4D) atlas by fitting a voxelwise logistic regression model to all the registered segmentations. We choose the logistic model to represent myelin maturation as it is the growth function with the smallest number of parameters. Lastly, the atlas is utilized to estimate the gestational ages of individual subjects in a leave-one-out procedure. We show that the logistic model obtains better estimation results compared to those predicted by a commonly used kernel regression method [3].

2. METHODS

2.1. Subjects and image acquisition

Preterm infants without brain injuries were scanned between 29 and 44 weeks gestational age (GA) at Hammersmith Hospital, London, UK with ethical approval. 96 T_2w fast spin-echo brain images were acquired on a 3T Philips Intera system with repetition time = 8700 ms, echo time = 160 ms and voxel sizes = 0.86 mm$\times$0.86 mm$\times$1 mm.

2.2. Segmentation of the tissue likely to contain myelin

The first step is to remove non-brain tissues using label propagation [4]. Segmentations of basal ganglia and thalami (BGT) and brainstem (BS) as well as bias corrected T_2w images are obtained using the Statistical Parametric Mapping (SPM) software[1] (version SPM8) [5] and a 4D probabilistic neonatal brain atlas[2] [3]. We choose BGT and BS to form a region of interest (ROI) because myelination in the perinatal period mainly occurs in these regions [6] and the ROI helps to simplify the segmentation problem.

We employ an expectation-maximization (EM) framework to segment the tissue likely to contain myelin in the ROI. We explicitly model partial volume (PV) voxels via second-order Markov random fields (MRFs) [7]. These PV voxels contain a mixture of tissue types and substantially distort the intensity distributions of the composing tissues. We define the following classes in each of the regions of BGT and BS: i) tissue likely to contain myelin; ii) background tissue; iii) PV voxels between the two defined classes. We apply the EM algorithm as follows:

Thanks to the University of Oxford Clarendon Fund Scholarship.

[1]http://www.fil.ion.ucl.ac.uk/spm
[2]http://www.brain-development.org

- E-step. We calculate the probability p_{ik} that voxel i belongs to class k:

$$p_{ik}^{(m+1)} = \frac{G(y_i, \mu_k^{(m)}, \sigma_k^{(m)}) p_{ik}^{\text{Anat}} e^{-U_{ik}^{2\text{nd}(m)}}}{\sum_{l=1}^{K} \left(G(y_i, \mu_l^{(m)}, \sigma_l^{(m)}) p_{il}^{\text{Anat}} e^{-U_{il}^{2\text{nd}(m)}} \right)} \quad (1)$$

The conditional distribution of class k is a Gaussian function of mean μ_k and standard deviation σ_k. Symbol y_i is the observed intensity, m the iteration number and K the total number of classes. We use the spatial anatomical prior p_{ik}^{Anat} to distinguish between the classes in the regions of BGT and BS and to prevent dense grey matter in caudate heads and lentiform nuclei being misclassified as myelin due to their similar signal properties. The second-order MRF penalty $U_{ik}^{2\text{nd}}$ is computed as follows:

$$U_{ik}^{2\text{nd}} = \sum_{k_1=1}^{K} \left(v_{k_1} \sum_{k_2=1}^{K} \mathbf{T}_k(k_1, k_2) v_{k_2} \right) \quad (2)$$

$$\text{where } v_k = \sum_{j \in N_i} \frac{p_{jk}}{d_{ij}} \quad (3)$$

Here N_i is the 26-neighbourhood of voxel i, p_{jk} the probability that neighbour j belongs to class k and d_{ij} the Euclidean distance between voxel i and the neighbour j. $\mathbf{T}_k(k_1, k_2)$ is the element of a 3D connectivity tensor [7] that represents the penalty when classes k_1 and k_2 are both present in the neighbourhood of class k. We configure the tensor so that PV voxels are only allowed if the tissue likely to contain myelin and the background tissue are both present in the neighbourhood.

- M-step. We optimize the log-likelihood function by assuming equal standard deviations for all the classes. Additionally, we assume that the myelin classes in the regions of BGT and BS have identical means and we approximate each of the PV classes with a single Gaussian function whose mean equals the average of the composing tissue means.

We obtain the final segmentation for the tissue likely to contain myelin by converting the posterior probability maps to the fractional content of the tissue likely to contain myelin. First we calculate the hard segmentations of the classes using the maximum-vote rule. Voxels voted as the myelin classes are assigned a fraction of one, and zero for the BGT and BS classes. For the PV voxels, we calculate the fractional content of the tissue likely to contain myelin f_i^S at voxel i in each individual subject's space as:

$$f_i^S = \frac{\mu_k - y_i}{\mu_k - \mu_{\text{myelin}}} \quad \text{for } k = \text{BGT or BS} \quad (4)$$

2.3. Spatio-temporal modelling of the tissue likely to contain myelin

We register the 96 T_2w images to the dilated ROI of a reference image using affine followed by non-rigid transformations [8]. Individual segmentations showing the fractional content of the tissue likely to contain myelin are then transformed accordingly from each subject's space to the common reference space.

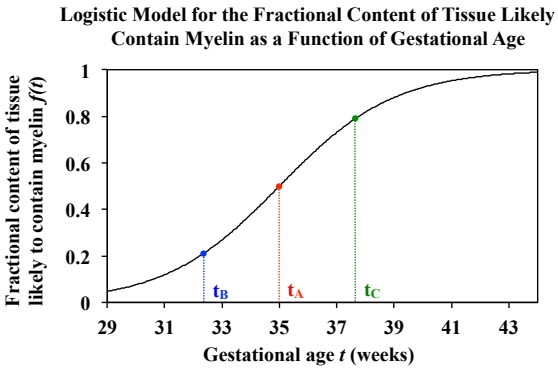

Fig. 1. Logistic model for the fractional content of the tissue likely to contain myelin $f(t)$ dependent on the gestational age t. The value of γ in Eq. 5 has been set to one. The age t_A represents the time point associated with the maximum slope of the function, t_B and t_C the time points associated with the maximum and minimum curvatures respectively.

To simulate the spatio-temporal progress of myelination, we fit the following voxelwise logistic regression model to the registered segmentations at each voxel i in the reference space:

$$f_i^A(t) = \frac{\gamma_i}{1 + e^{-(\alpha_i + \beta_i t)}} \quad (5)$$

Symbol f_i^A is the fractional content of the tissue likely to contain myelin in the reference space and t the gestational age. The parameters α and β together define the time point t_A associated with the maximum slope of the logistic function:

$$\frac{\mathrm{d}f}{\mathrm{d}t}\Big|_{max} = \frac{\gamma\beta}{4} \text{ at } t_A = -\frac{\alpha}{\beta} \quad (6)$$

We consider t_A a critical time point because it is the age when the anatomical location myelinates on average. The parameter γ estimates the final fraction of the tissue likely to contain myelin when myelination has completed. This logistic model is illustrated in Fig. 1. We optimize the parameters α, β and γ at each location via a Levenberg-Marquardt nonlinear least squares algorithm [9]. A 4D spatio-temporal atlas based on all the 96 segmentations of the tissue likely to contain myelin is then created using the fitted model. Moreover, we construct a 3D map of the critical age t_A to investigate the myelination timetable of preterm brains.

When constructing the 4D atlas and the parameter map, we use the voxels only if the fitted function is consistent with the expected increase of the myelin content in time. We require that $24 \leq t_A \leq 43$ because according to Counsell *et al.* [6], myelination in the ROI occurs the earliest at 25 weeks GA and the latest at 42 weeks GA for preterm neonates. Additional constraints that $\beta > 0$ and $\gamma \geq 0.5$ are included to

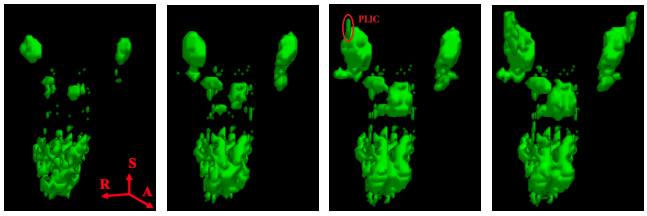

Fig. 2. 4D atlas of the tissue likely to contain myelin (binarized at a fraction of 0.5) at ages of 30, 35, 40 and 44 weeks GA shown from left to right. The logistic model suggests that the posterior limb of internal capsule (PLIC) becomes myelinated at approximately 40 weeks GA. This is an important signature on T_2w images consistent with clinically observed myelination.

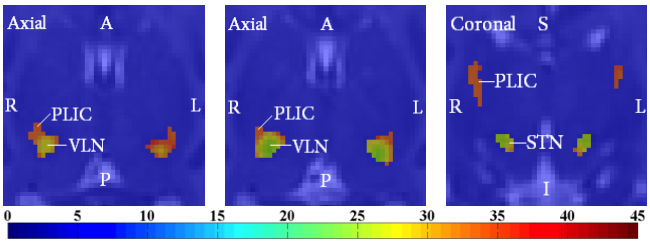

Fig. 3. 3D map of the critical age t_A shown in axial and coronal views, superimposed on the reference T_2w image. This map confirms the signature revealed in Fig. 2 that the PLIC becomes myelinated by the age of 40 weeks GA. Abbreviations: PLIC-posterior limb of internal capsule, VLN-ventrolateral nuclei, STN-subthalamic nuclei.

ensure that the function is monotonically increasing and that sufficient myelination has occurred at the location. We discard the voxels that do not fulfil the constraints.

2.4. Estimation of gestational ages

We estimate the gestational ages of the subjects by fitting the voxelwise logistic regression model described in Section 2.3 in a leave-one-out procedure. The 4D atlas is now created for each subject based on the remaining 95 segmentations. We find the estimated age of the test subject by minimizing the sum of squared differences (SSD) between the atlas and the individual segmentation with respect to the gestational age t:

$$SSD(t) = \frac{1}{n}\sum_{i=1}^{n}\left(\frac{\gamma_i}{1+e^{-(\alpha_i+\beta_i t)}} - s_i\right)^2 \qquad (7)$$

Here n is the number of voxels considered and s_i the segmentation value at voxel i of the subject.

We impose more restricted conditions for age estimation by calculating the time points t_B and t_C associated with the maximum and minimum curvatures respectively (Fig. 1):

$$t_{B,C} = -\frac{\ln(2\pm\sqrt{3})+\alpha}{\beta} \qquad (8)$$

The SSD is evaluated only at the voxels where the values of t_B and t_C are both within the age range of the image data. Therefore, we replace the constraint that $24 \le t_A \le 43$ with $t_B \ge 29$ and $t_C \le 44$ while the other conditions remain unchanged.

3. EXPERIMENTS AND RESULTS

3.1. 3D map of the critical age t_A

Automatic segmentations of the tissue likely to contain myelin were validated for 16 representative subjects between 29 and 44 weeks GA against manual annotations. The average Dice overlap between the automatic and manual segmentations was 0.821($\pm$0.040). We non-rigidly registered all the segmentations from each individual subject's space to the reference space of a subject at 36 weeks GA and performed the logistic regression analysis as explained in Section 2.3.

We present the 4D atlas of the tissue likely to contain myelin in Fig. 2. The 3D map of the critical age t_A is shown in Fig. 3. The modelling results confirmed the myelination timetable described by Counsell *et al.* [6] for preterm neonates. For example, the logistic model suggests that the posterior limb of internal capsule (PLIC) becomes myelinated by the age of 40 weeks GA. This is an important signature of myelination on T_2w images consistent with clinical knowledge. The quality of model fitting was confirmed by the average error between the 4D atlas and individual segmentations. The value averaged over all the subjects and all the selected voxels was 0.025.

3.2. Comparing the logistic and kernel regression models for age estimation

We constructed the 4D atlas of the tissue likely to contain myelin in a leave-one-out fashion for each subject and used the atlas to estimate the gestational age of the test subject. The estimation results are plotted in Fig. 4. The logistic model produced a root mean squared error of 10 days according to

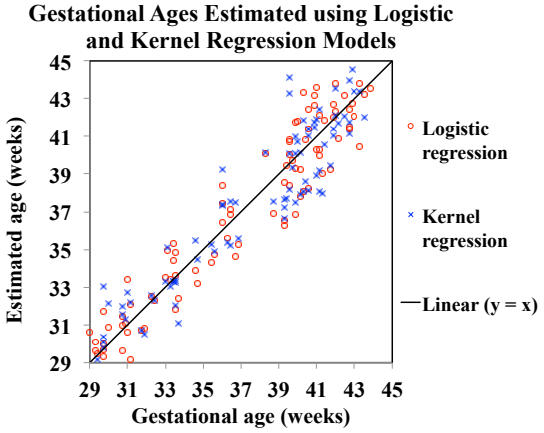

Fig. 4. Comparison between the logistic and kernel regression models. The straight line $y = x$ shows the true gestational ages in the clinical record.

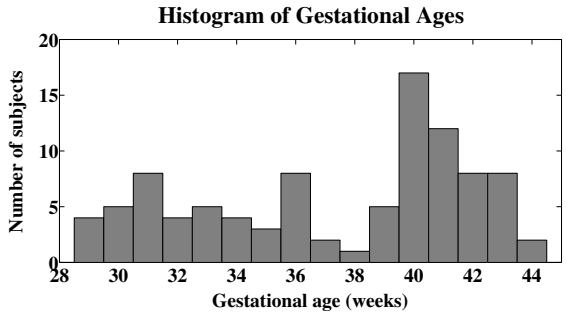

Fig. 5. Subject distribution according to their gestational ages. The peak at the age of 40 weeks GA is due to the fact that preterm infants are usually examined at birth followed by another scan at term in clinical practice.

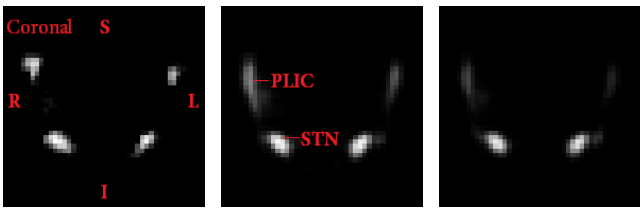

(a) (b) (c)

Fig. 6. (a) Segmentation of the tissue likely to contain myelin in a subject at 39.3 weeks GA. (b) 4D atlas showing the fractional content of the tissue likely to contain myelin at 39.3 weeks GA, constructed using kernel regression. Unlike Fig. (a), the tissue is present throughout the PLIC tract. This discrepancy is due to the large number of 40-week-old subjects that make the atlas appear more mature near 39 weeks. As a result, the subject's age is under-estimated. (c) The kernel regression atlas at the under-estimated age of 37.7 weeks. See Fig. 3 for the abbreviations.

the true ages in the clinical record, as compared to 13 days for the ages predicted using a kernel regression method [3].

We found that the logistic model was less affected by the non-uniform subject distribution (Fig. 5) compared to kernel regression where the 4D atlas was constructed non-parametrically by summing weighted segmentations. Each weight was calculated using a Gaussian function of one-week standard deviation. Consequently, the kernel regression atlas near 39 weeks GA appeared falsely more mature due to the adjacent large 40-week-old cohort, causing under-estimation of the ages (Fig. 6).

4. CONCLUSION

The contribution of this work is to present a method that helps assess brain maturation of preterm neonates using routinely acquired clinical MRI. We developed a spatio-temporal growth model for the tissue likely to contain myelin and predicted the gestational ages of subjects between 29 and 44 weeks GA with expected accuracy. In the future, we will improve the registration by using an average reference space and consider other growth models such as the adaptive kernel regression [10] for comparison. We will also incorporate T_1w images for enhanced segmentation.

5. REFERENCES

[1] J. Dubois, G. Dehaene-Lambertz, Kulikova S., C. Poupon, P.S. Huppi, and L. Hertz-Pannier, "The early development of brain white matter: A review of imaging studies in fetuses, newborns and infants," *Neuroscience*, vol. 276, pp. 48–71, 2014.

[2] M.A. Rutherford, *MRI of the Neonatal Brain*, Saunders, Edinburgh, 2002.

[3] M. Kuklisova-Murgasova, P. Aljabar, L. Srinivasan, S.J. Counsell, V. Doria, A. Serag, I.S. Gousias, J.P. Boardman, M.A. Rutherford, A.D. Edwards, J.V. Hajnal, and D. Rueckert, "A dynamic 4D probabilistic atlas of the developing brain," *NeuroImage*, vol. 54, pp. 2750–2763, 2011.

[4] R.A. Heckemann, J.V. Hajnal, P. Aljabar, D. Rueckert, and A. Hammers, "Automatic anatomical brain MRI segmentation combining label propagation and decision fusion," *NeuroImage*, vol. 33, pp. 115–126, 2006.

[5] J. Ashburner and K.J. Friston, "Unified segmentation," *NeuroImage*, vol. 26, pp. 839–851, 2005.

[6] S.J. Counsell, E.F. Maalouf, A.M. Fletcher, P. Duggan, M. Battin, H.J. Lewis, A.H. Herlihy, A.D. Edwards, G.M. Bydder, and M.A. Rutherford, "MR imaging assessment of myelination in the very preterm brain," *Am. J. Neuroradiol.*, vol. 23, pp. 872–881, 2002.

[7] C. Ledig, R. Wright, A. Serag, P. Aljabar, and D. Rueckert, "Neonatal brain segmentation using second order neighborhood information," in *Proceedings of the MICCAI Workshop: Perinatal and Paediatric Imaging*, 2012, pp. 33–40.

[8] D. Rueckert, L.I. Sonoda, C. Hayes, D.L.G. Hill, M.O. Leach, and D.J. Hawkes, "Nonrigid registration using free-form deformatins: Application to breast MR images," *IEEE Trans. Med. Imag.*, vol. 18, no. 8, pp. 712–721, 1999.

[9] K. Levenberg, "A method for the solution of certain problems in least-squares," *Q. Appl. Math.*, vol. 2, pp. 164–168, 1944.

[10] A. Serag, P. Aljabar, G. Ball, S.J. Counsell, J.P. Boardman, M.A. Rutherford, A.D. Edwards, J.V. Hajnal, and D. Rueckert, "Construction of a consistent high-definition spatio-temporal atlas of the developing brain using adaptive kernel regression," *NeuroImage*, vol. 59, pp. 2255–2265, 2012.